SHORT THESIS FOR THE DEGREE OF DOCTOR OF PHYLOSOPHY (Ph.D.)

MOLECULAR ORGANIZATION OF THE ENDOCANNABINOID SYSTEM IN THE SPINAL DORSAL HORN OF RODENTS

Zoltán Hegyi

Supervisor: Miklós Antal MD, PhD, DSc

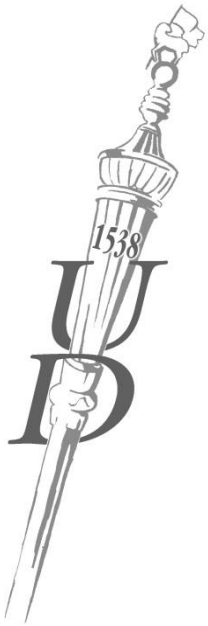

UNIVERSITY OF DEBRECEN

DOCTORAL SCHOOL OF NEUROSCIENCES

DEBRECEN, 2013.

INTRODUCTION

Between 50 and 70 AD, a Greek physician, pharmacologist and botanist Pedanius Dioscorides wrote a five-volume book *De Materia Medica*, in which he described the use of more than 500 medicinal plants to cure certain diseases. This collection has been an inexhaustible source of drugs for more than 19 centuries, still containing powerful and effective medicinal plants with unknown mechanisms of action.

In 1962, Raphael Mechoulam, the young postdoctoral fellow at the Hebrew University in Jerusalem, decided to investigate one of the famous and promising plants in Dioscorides' Herbal: the Cannabis sativa, also known as the hemp, one of the most widely used drugs throughout the world. In two years, the major psychoactive component of the Cannabis has successfully been identified and named delta-9-tetrahydrocannabinol or THC (Gaoni and Mechoulam, 1964). As it turned out, the chemical structure of THC is remarkably different from the other plant-derived compounds. Based on its strong hydrophobic nature, THC was thought to act by influencing the biophysical properties of cell membranes rather than via specific interactions with selective binding sites.

More than 20 years later, experiments with highly selective, enantiomerically pure THC analogues showed that their major pharmacological actions are enantioselective, and mediated by inhibiting cAMP accumulation (Howlett and Fleming, 1984). These findings suggested the existence of cannabinoid-binding receptor, which was identified and cloned only in 1990 by Matsuda and his co-workers (Matsuda *et al.*, 1990). The discovery of cannabinoid receptor (CB1-R) helped to explain the pharmacological effects of THC, but raised questions regarding the brain-derived, endogenous ligands of CB1-R. To the greatest surprise, in the early '90s not only one but two cannabimimetic compounds have been isolated: anandamide (arachidonoyl-ethanolamide; Devane et al, 1992) and 2-AG (2-arachidonoyl-glycerol; Mechoulam et al, 1995; Sugiura et al, 1995). In the past 20 years, biosynthetic and catabolic pathways and ezymes for anandamide and 2-AG, as well as additional cannabinoid sensitive receptors and an entire family of endogenous cannabinoid ligands have been elucidated. The cannabinoid-related endogenous ligands, their

anabolic and catabolic enzymes and receptors together are regarded as the endocannabinoid system.

Although Cannabis has been used for centuries as a recreational drug, it was also prescribed as medicine against pain and spasm. However, biomedical research has only recently been focusing on the Cannabis' true therapeutic potential and the unexpectedly powerful endocannabinoid influence on different physiological and pathological functions, from cancer and epilepsy to fertility and obesity (Pacher et al, 2006.). One of the most interesting observations is that both exogenous cannabinoid compounds and endocannabinoid ligands effectively induce antinociception, which in potency and efficacy is comparable to the analgesic effects of morphine (Bloom et al, 1977). It has been demonstrated, that the molecular players of the endocannabinoid system, primarily the CB1-Rs are localized at mutiple levels of the pain pathways suggesting that the endocannabinoid system may modulate pain processing at peripheral, spinal and supraspinal levels (Herkenham et al, 1991; Pertwee, 2001; Agarwal et al, 2007; Drew et al, 2008).

Considering the well-known gate control theory of pain, which has been proposed by Melzack and Wall (Melzack and Wall, 1965), neural networks in the dorsal horn of the spinal cord can be regarded as the primary area of the central nervous system that can effectively modulate nociceptive information processing. CB1-Rs are strongly expressed in the spinal dorsal horn, as it has been reported in immunocytochemical (Farquhar-Smith et al, 2000) and in situ hybridization studies (Mailleux and Vanderhaeghen, 1992). These molecular anatomical data helped to explain the cannabinoid-evoked antinociception after intrathecal administration of the cannabinoid agonist WIN 55,212-2 (Hohmann et al, 1995), as well as the cannabinoid-mediated suppression of C- and Aδ-fiber evoked responses in dorsal horn neurons (Strangman and Walker, 1999; Kelly and Chapman, 2001). However, the laminar distribution and cellular localization of CB1-Rs in laminae I-II of the spinal dorsal horn, which contains the primary pain processing neural network, remains controversial (Hohmann et al, 1999; Ong and Mackie, 1999; Salio et al, 2001, 2002; Farquhar-Smith et al, 2000).

Causing further difficulties in the understanding of the spinal endocannabinoid system, surprisingly little is known about the molecular anatomical background of the endocannabinoid mobilization at the level of the spinal cord. Nyilas et al. (2009) provided convincing experimental evidence for the ultrastructural localization of diacylglycerol lipase alpha (DGL-α), the synthesizing enzyme of 2-

AG. However, the distribution of DGL-α among the cellular elements of the spinal cord remains largely unknown.

Investigation of the morphological substrate of anandamide biosynthesis could be even more complicated, since no less then five paralell metabolic pathways are involved in the biogenesis of N-acyethanolamides (Sun et al, 2004; Simon and Cravatt, 2006, 2008; Liu et al, 2006), the most important and best known being catalyzed by N-acylphosphatidylethanolamine-specific phospholipase D (NAPE-PLD; Okamoto et al, 2004). Previous studies have reported that NAPE-PLD is localized predominantly to intracellular membrane cisternae of axonal calcium strores (Egertova et al, 2008; Nyilas et al, 2008). However, experimental evidence for the somatodendritic localization of NAPE-PLD has also been provided (Cristino et al, 2008). To date, however, expression of NAPE-PLD in the spinal dorsal horn has not been investigated, thus the morphological background of spinal anandamide mobilization remains completely unknown.

MAJOR AIMS

Although a great body of literature suggests the functional importance of cannabinoid mechanisms in the modulation of spinal pain processing, the molecular architecture of the endocannabinoid signaling machinery in the spinal dorsal horn is significantly less well studied than that of the cerebral cortex or hippocampal formation. The objective of this study was to provide a detailed molecular anatomical description of key elements of the endocannabinoid system in the supeficial dorsal horn of the rodent's spinal cord.

Therefor, the major aims of our studies were the followings:

- to describe the cellular distribution and subcellular localization of CB1-Rs in the superficial spinal dorsal horn
- to provide an accurate description of cellular expression and ultrastructural localization of DGL-α and NAPE-PLD in laminae I-II of the spinal cord
- to investigate the expression of molecular elements of the endocannabinoid signaling apparatus by glial cells in the superficial spinal dorsal horn.

MATERIALS AND METHODS

Animals and preparation of tissue sections

Experiments were carried out on 17 adult rats (Wistar-Kyoto, 250‑300 g, Gödöllő, Hungary) and four wild-type, two CB1-R knockout and one NAPE-PLD knockout mice. All animal study protocols were approved by the Animal Care and Protection Committee at the University of Debrecen, and were in accordance with the European Community Council Directives and the rules of the Indiana University Institutional Animal Care and Use Committee. Fourteen animals were deeply anesthetized with sodium pentobarbital (50 mg/kg, i.p.) and transcardially perfused with Tyrode's solution (oxygenated with a mixture of 95% O_2, 5% CO_2), followed by a fixative containing either (1) 4% paraformaldehyde (three adult rats and all mice; for peroxidase based single and fluorescent double immunostaining), (2) 4% paraformaldehyde and 0.1% glutaraldehyde (three adult rats; for preembedding immunostaining for electronmicroscopy in case of DGL-α or NAPE-PLD localization studies) or (3) 2.5% paraformaldehyde and 0.5% glutaraldehyde (for peroxidase- and nanogold-based immunohistochemistry for electron microscopy in case of CB1-R localization studies) dissolved in 0.1 M phosphate buffer (PB, pH 7.4).). In three additional animals 2 weeks prior to the transcardial perfusion, the lumbar spinal cord was exposed by laminectomy and the L2‑S1 spinal dorsal roots were cut unilaterally under deep sodium pentobarbital anesthesia.

After the transcardial fixation, the L3-L5 lumbar segments of the spinal cord were removed, postfixed in their original fixative for 1 to 4 hours, and immersed into 10% and 20% sucrose dissolved in 0.1 M PB until they sank. In order to enhance reagent penetration the removed spinal cord was freeze-thawed in liquid nitrogen. Fifty-micrometer thick transverse sections were cut on a vibratome, and the sections were extensively washed in 0.1 M PB.

Immunohistochemistry

Single immunostaining protocols were performed to study the laminar distribution of CB1-R, DGL-α and NAPE-PLD. Free-floating sections were first incubated in (1) rabbit anti-CB1-R antibody (1:5,000), (2) rabbit anti-DGL-α (1:1,000) or (3) guinea pig anti-NAPE-PLD antibody (1:200) for 48 h at 4 °C, and then were transferred into biotinylated goat anti-rabbit IgG or goat anti-guinea pig IgG (1:200) for 12 h at 4 °C. Thereafter, the sections were treated with an avidin biotinylated horseradish peroxidase complex (1:100) for 5 h at room temperature, and the immunoreaction was completed with a 3,3'-diaminobenzidin chromogen reaction. Before the antibody treatments the sections were kept in 10% normal goat serum for 50 min. Sections were mounted on glass slides, dehydrated and covered with Permount neutral medium.

Double-immunostaining protocols were performed to study the co-localization of CB1-R , DGL-α and NAPE-PLD immunoreactivity with various markers of nociceptive primary afferents, axon terminals of putative glutamatergic and GABAergic spinal neurons, astrocytes, and microglial cells. Free-floating sections were first incubated with a mixture of antibodies that contained rabbit anti-CB1-R (1:5,000), rabbit anti- DGL-α (1:1,000) or guinea pig anti-NAPE-PLD antibody (1:200) and one of the following antibodies: (1) guinea pig anti-calcitonin gene-related peptide (CGRP; 1:2,000), (2) rabbit anti-calcitonin gene-related peptide (CGRP; 1:10,000), (3) biotinylated isolectin B4 (IB4; 1:2,000), (4) guinea pig anti-vesicular glutamate transporter 2 (VGLUT2; 1:2,000), (5) mouse anti-vesicular glutamate transporter 2 (1:10,000), (6) a mixture of mouse anti-glutamic acid decarboxylase 65 and mouse anti-glutamic acid decarboxylase 67 (GAD65 and GAD67; 1:1,000), (7) mouse anti-glial fibrillary acidic protein (GFAP; 1:1,000) and (8) mouse anti-CD11b (1:500).

The sections were incubated in the primary antibody solutions for 2 days at 4 °C and were transferred for an overnight treatment into the appropriate mixtures of secondary antibodies that were selected from the following: (1) goat anti-rabbit IgG conjugated with Alexa Fluor 555 (1:1,000), (2) goat anti-guinea pig IgG conjugated with Alexa Fluor 488 (1:1,000), (3) goat anti-mouse IgG conjugated with Alexa Fluor 488 (1:1,000), (4) goat anti-guinea pig IgG conjugated with Alexa Fluor 555 (1:1,000), (5) goat anti-rabbit IgG conjugated with Alexa Fluor 488 (1:1,000) and (6) streptavidin conjugated with Alexa Fluor 488 (1:1,000).

Before the antibody treatments the sections were kept in 10% normal goat serum for 50 min. Sections were mounted on glass slides and covered with Vectashield.

Confocal microscopy and analysis

Series of 1 μm thick optical sections with 0.3 μm separation in the z-axis were scanned with an Olympus FV1000 confocal microscope. Scanning was carried out using a 60x oil-immersion lens (NA: 1.4). The confocal settings (laser power, confocal aperture, and gain) were identical for all sections, and care was taken to ensure that no pixels corresponding to puncta immunostained for each marker applied for the visualization of nociceptive primary afferents, axon terminals of glutamatergic and GABAergic spinal neurons, astrocytes and microglial cells were saturated. The scanned images were processed by Adobe Photoshop CS5 software. By filtering the background staining out with a high-pass intensity filter, threshold values were set for each marker.

The co-localization of CB1-R, DGL-α and NAPE-PLD with the investigated markers was quantitatively analyzed in the double-stained sections. A 10x10 standard square grid in which the edge-length of the unit square was 4 μm (the whole grid was 40 μm x 40 μm in size) was placed onto the regions of confocal images corresponding to laminae I–II of the superficial spinal dorsal horn. The proper placement of the grid was based on the following criteria: (a) the border between the dorsal column and the dorsal horn was easily identified on the basis of the intensity of immunostaining, and (b) the border between laminae II and III was approximated on the basis of previous ultrastructural observations. Thus, immunoreactivities and co-localizations were investigated in the most superficial 150 μm thick zone of the dorsal horn that had earlier been identified as a layer of the gray matter corresponding to laminae I and II in the L3-L5 segments of the spinal dorsal horn. Profiles that showed immunoreactivity for CB1-R, DGL-α or NAPE-PLD over the edges of the standard grid were counted in the medial and lateral compartments of laminae I and II. The selected profiles were then examined whether they were also immunoreactive for the axonal or glial markers.

Since the CB1-R, DGL-α and NAPE-PLD antibodies utilized in the present study were raised against the intracellular domain of the enzyme, to define the colocalization values we counted only those CB1-R, DGL-α or NAPE-PLD immunolabeled puncta that were located within the confines of the areas immunostained for the marker. The co-localization for all investigated markers was

analyzed in three animals. The quantitative measurement was carried out in three sections that were randomly selected from each animal. Thus, the calculation of quantitative figures, mean values and standard error of means (SEM), was based on the investigation of nine sections.

The numbers of CB1-R- and VGLUT2-immunoreactive puncta in laminae I and IIi at the level of L4 spinal segment were quantitatively analysed in control animals and in animals with dorsal rhizotomy. A 10 x 10 standard square grid with an edge-length of 4 μm was put onto confocal images obtained from 1-μm-thick single optical sections. CB1-R- and VGLUT2-immunoreactive puncta over the edges of the standard grid were counted in the medial and lateral compartments of laminae I and IIi. The quantitative measurement was carried out in three control animals and in three animals with dorsal rhizotomy. Three randomly selected confocal sections were analysed from each animal. Thus the calculation of quantitative figures was based on the investigation of nine sections. From quantitative data obtained in the nine sections mean values and standard error of the means (SEM) were calculated. Data obtained from control animals and from animals with dorsal rhizotomy were compared. Statistical differences between experimental groups were determined using a one-way Anova test. Probabilities (P) of <0.05 were considered to be statistically significant.

Preembedding immunostaining with diaminobenzidine chromogen reaction for electron microscopy

A preembedding immunostaining similar to the single immunostaining protocol described above was performed to study the cellular distribution of DGL-α and NAPE-PLD at the ultrastructural level. Following extensive washes in 0.1 M PB and a treatment with 1% sodium borohydride for 30 min, free-floating sections from animals fixed with 4% paraformaldehyde and 0.1% glutaraldehyde were first incubated with rabbit anti-DGL-α (1:1,000) or guinea pig anti-NAPE-PLD antibody (1:200) for 48 h at 4 °C, than were transferred into biotinylated goat anti-rabbit IgG or goat anti-guinea pig IgG (1:200) for 12 h at 4 °C. Thereafter, the sections were treated with an avidin biotinylated horseradish peroxidase complex (1:100) for 5 h at room temperature, and the immunoreaction was completed with a 3,3’-diaminobenzidine chromogen reaction. Before the antibody treatments the sections were kept in 10% normal goat serum for 50 min.

Immunostained sections were treated with 0.5% osmium tetroxide for 45 min, then dehydrated and flat-embedded into Durcupan ACM resin on glass slides. Selected sections were re-embedded, ultrathin sections were cut and collected on Formvar-coated single-slot nickel grids, and counterstained with uranyl acetate and lead citrate.

Preembedding nanogold immunostaining for electron microscopy

A preembedding nanogold immunohistochemical protocol was performed to study the cellular distribution of CB1-R, DGL-α and NAPE-PLD with high resolution. Following extensive washes in 0.1 M PB and treatment with 1% sodium borohydride for 30 min, free-floating sections from animals fixed with 2.5% paraformaldehyde and 0.5% glutaraldehyde were incubated in rabbit anti-CB1-R antibody (1 : 2,500), whereas sections from rats perfused with 4% paraformaldehyde and 0.1% glutaraldehyde were treated with rabbit anti-DGL-α (1:1,000) or guinea pig anti-NAPE-PLD antibody (1:200) for 48 h at 4 °C. The sections were then transferred into a solution of goat anti-rabbit or goat anti-guinea pig IgG conjugated to 1-nm gold particles (1:100) for 12 h at 4 °C.

After repeated washing in 0.01 M Tris-buffered isotonic saline (TBS), the sections were postfixed for 10 min in 2.5% glutaraldehyde and washed again in 0.01 M TBS and 0.1 M PB. The gold labeling was intensified with a silver enhancement reagent. Sections were treated with 1% osmium tetroxide for 45 min, then dehydrated and flat-embedded into Durcupan ACM resin on glass slides. Selected sections were re-embedded, ultrathin sections were cut and collected on Formvar-coated single-slot nickel grids, and counterstained with uranyl acetate and lead citrate.

Controls

To test the specificity of the antibody raised against CB1-R, free-floating sections obtained from CB1-R knock-out and wild-type mice were immunostained according to the single immunostaining protocol described above. Sections of CB1-R knockout mice were negative for CB1-R, whereas wild-type mice showed a characteristic immunostaining identical to that observed in rats.

To exclude false negative staining for CB1-R the double immunolabeling for CB1-R and CGRP was repeated using the anti-CB1-R antibody, which was originally diluted at 1:5,000, at a dilution of 1:1,000. The co-localization of CB1-R with CGRP was quantitatively analysed as described

above. Levels of co-localization found with the lower and higher anti-CB1-R dilutions were compared. The two sets of co-localization values did not show any significant differences.

The specificity of the antibody against DGL-α spinal cord sections were double-immunostained with the antibody used in this study (epitope: 790-908 aa) and with another antibody raised against a different epitope of the DGL-α protein (epitope: 1001-1042 aa) that we purchased from the Frontier Institute Co. The two antibodies revealed identical immunostaining patterns.

To test the specificity of the antibody raised against NAPE-PLD, free-floating sections obtained from NAPE-PLD knock-out and wild-type mice were immunostained according to the single immunostaining protocol described above. Sections from the spinal cord of NAPE-PLD knock-out mice were negative for NAPE-PLD, whereas wild-type littermates showed a characteristic immunostaining identical to that observed in rats.

To obtain a more global view about the specificity of the anti-CB1, anti-DGL-α and anti-NAPE-PLD antibodies, Western-blot analyses were performed. While the rats were deeply anesthetized with sodium pentobarbital, the spinal dorsal horn at the level of L3-L5 lumbar segments were dissected. The dorsal horn was sonicated in 20 mM Tris lysis buffer containing the following protease inhibitors: EDTA, EGTA, PMSF, benzamidine, pepstatine A, soybean trypsine inhibitor, leupeptine and aprotinin. After removing cell debris from the sonicated samples with centrifugation, the supernatant was centrifuged again (12,000 g for 20 minutes at 4^{o}C). The pellet was re-suspended in lysis buffer containing 1% Triton X-100 and 0.1% SDS, and the samples were run on 10% SDS-polyacrylamide gels according to the method of Laemmli. The separated proteins were electrophoretically transferred onto PVDF membranes, and the membranes were immunostained according to the single immunostaining protocol described above. The immunostaining revealed only one immunoreactive band at molecular weight of 53 kDa for CB1-R, 115 kDa for DGL-α and 46 kDa for NAPE-PLD corresponding to the molecular weight of CB1-R and the enzymes.

Since in our experiments IB4 was used as specific marker of non-peptidergic primary afferent terminals, we have to add, that in some of the earlier reports, IB4-binding to astrocytes and microglial cells has been demonstrated. In contrast to these reports, we have never seen IB4-binding on glial cells in the present study.

To test the specificity of the immunostaining protocol, free-floating sections were incubated according to the single immunostaining protocol described above with primary antibodies omitted or replaced with 1% normal goat serum. No immunostaining was observed in these sections.

RESULTS

Distribution of CB1-R immunoreactivity in the superficial spinal dorsal horn

Peroxidase-based single immunostaining revealed an abundant immunoreactivity for CB1-R in the lumbar spinal cord of rats that was mostly confined to a twin band corresponding to lamina I and the inner portion of lamina II (lamina IIi). The two heavily stained bands were separated by a narrow zone corresponding to the outer portion of lamina II (lamina IIo), where only a sparse immunostaining was observed. Immunostained elements appeared exclusively as punctuate profiles in both the densely and the sparsely stained zones.

Somatic or dendritic immunostaining was never observed in laminae I and II. This pattern of immunostaining was characteristic of laminae I and II throughout the rostro-caudal extent of the lumbar spinal cord with the exception of segment L4 and the adjacent territories of segments L3 and L5. At this level lamina IIi showed an intense immunostaining only in the lateral aspect of the dorsal horn, whereas the staining intensity in the medial aspect of lamina IIi was similar to that observed in lamina IIo (Fig. 13b). At his level of the spinal cord, the medial aspect of the dorsal horn receives high number of primary afferent inputs from the plantar surface of the hind paw, which makes the inner portion of lamina II less compact (Molander & Grant, 1985, 1986), thus the density of CB1-R immunoreactivity appears to be decreased. Otherwise, the distribution of immunoreactivity for CB1-R at the level of the L4 spinal segment was similar to that in other segments of the lumbar spinal cord.

Co-localization of CB1-R immunoreactivity with markers of nociceptive primary afferents

There is general agreement that synaptic transmission from a population of the nociceptive primary afferents is mediated only by glutamate, whereas others, in addition to glutamate also release neuropeptides. Most of the peptidergic nociceptive primary afferents express CGRP, whereas the cell-coat of the non-peptidergic axon terminals contains a polysaccharide that selectively binds the lectin isolated from Bandeiraea simplicifolia, IB4. Thus, to study the expression of CB1-Rs on central axon terminals of peptidergic and non-peptidergic nociceptive primary afferents we investigated the co-localization of CB1-Rs with CGRP immunoreactivity and IB4 binding.

In agreement with previous studies, we observed a strong immunostaining for CGRP in laminae I–IIo. Investigating the co-localization between CB1-R and CGRP immunoreactivity, we found that 16.74 ± 1.55 and 18.15 ± 0.84% (when the CB1-R antibody was diluted 1:5,000), and 17.62 ± 0.77 and 17.49 ± 0.87% (when the CB1-R antibody was diluted 1:1000) of CB1-R-immunoreactive puncta were also stained for CGRP, whereas 46.36 ± 2.54 and 49.10 ± 0.80% (when the CB1-R antibody was diluted 1:5,000), and 44.35 ± 2.31 and 47.51 ± 0.68% (when the CB1-R antibody was diluted 1:1,000) of CGRP-immunoreactive axon terminals proved to be immunoreactive also for CB1-R in the medial and lateral aspects of the dorsal horn, respectively.

As has been reported previously, IB4 binding labeled a large number of axon terminals in lamina IIi. Although the intensity of CB1-R immunostaining was strikingly different in the medial and lateral aspects of lamina IIi, the co-localization between CB1-R immunoreactivity and IB4 binding was surprisingly similar in the medial and lateral compartments: 21.56 ± 1.48 and 18.55 ± 0.92% of CB1-R-immunoreactive puncta were also positive for IB4 binding, whereas 20.94 ± 1.72 and 21.66 ± 1.56% axon terminals that were positive for IB4 binding proved to be immunoreactive also for CB1-R in the medial and lateral aspects of the dorsal horn, respectively.

Co-localization of CB1-R immunoreactivity with markers of axon terminals of glutamatergic and GABAergic spinal neurons

Much experimental evidence in recent years suggests that VGLUT2 can be used as a marker for axon terminals of intrinsic spinal neurons. However, it is also accepted that GABAergic neurons synthesize GABA with the aid of GAD. All GABAergic neurons in the spinal cord are thought to contain both isoforms of GAD (GAD65 and GAD67, although the relative amounts of the two enzymes vary widely, with some cells expressing predominantly GAD65 and others mainly GAD67. Therefore, to study the expression of CB1-Rs on central axon terminals of glutamatergic and GABAergic spinal neurons we investigated the co-localization between CB1-R and VGLUT2 as well as GAD65/67 immunoreactivities.

Confirming results of previous studies, VGLUT2-immunoreactive axon terminals were homogeneously distributed in laminae I–II. Despite the contrasting distribution of CB1-R immunoreactivity in the medial and lateral aspects of lamina I–II, the co-localization between CB1-R and VGLUT2 immunoreactivity was very similar throughout the entire medio-lateral extent of the superficial spinal dorsal horn. It was found that 28.93 ± 0.70 and 28.71 ± 1.19% of CB1-R-

immunoreactive puncta were also immunostained for VGLUT2, whereas 33.60 ± 1.34 and 36.28 ± 0.96% axon terminals that were positive for VGLUT2 were also immunoreactive for CB1-R in the medial and lateral aspects of the dorsal horn, respectively.

Dorsal rhizotomy at the level of spinal segments L2–S1 caused a slight reduction in the number of VGLUT2-immunoreactive puncta in the superficial dorsal horn of the L4 spinal segment. Counting VGLUT2 immunoreactive puncta along the edges of a standard square grid, on average there were 44.6 ± 2.2 and 42.1 ± 1.7 puncta per grid in laminae I and IIi of control animals, respectively. In animals with dorsal rhizotomy, these values were 41.5 ± 1.5 and 39.7 ± 1.0 in laminae I and IIi, respectively. Thus, the loss of primary afferents terminating in the superficial spinal dorsal horn resulted in a noticeable but non-significant 8.52% (p=0.3645) and 5.73% (p=0.3600) decrease in the total numbers of VGLUT2-immunoreactive puncta in laminae I and IIi, respectively. The loss of VGLUT2-immunoreactive primary afferents did not cause any substantial change in the co-localization of CB1-R and VGLUT2 immunoreactivities either. In animals with dorsal rhizotomy, 26.94 ± 0.41 and 25.49 ± 0.76% of CB1-R-immunoreactive puncta were also immunostained for VGLUT2, whereas 36.40 ± 1.21 and 35.50 ± 1.63% axon terminals that were positive for VGLUT2 were also immunoreactive for CB1-R in the medial and lateral aspects of the dorsal horn, respectively. Statistical differences between the corresponding co-localization values of control animals and animals with dorsal rhizotomy were all non-significant; p-values were 0.50, 0.13, 0.25 and 0.78, respectively.

Similar to earlier reports, GAD65⁄67-immunoreactive axon terminals showed a dense and homogeneous distribution in the superficial spinal dorsal horn. Investigating the co-localization between CB1-R and GAD65⁄67 immunoreactivity, we found that 9.22 ± 1.01 and 10.88 ± 1.08% of CB1-R immunoreactive puncta were also stained for GAD65⁄67, whereas 22.22 ± 1.79 and 17.2 ± 0.89% of GAD65 ⁄ 67-immunoreactive axon terminals proved to be immunoreactive also for CB1-R in the medial and lateral aspects of the dorsal horn, respectively.

Co-localization of CB1-R immunoreactivity with markers of astrocytes and microglial cells

A great deal of experimental evidence has accumulated in recent years suggesting the existence of a bidirectional communication between glial cells and neurons. It has also been demonstrated that CB1-Rs are expressed by microglial cells in the cerebral cortex, and also by astrocytes in the hippocampus, caudate putamen nucleus and dorsal horn of the spinal cord. Direct

experimental evidence has also been provided that CB1-Rs on astrocytes can be activated by endocannabinoids released by neurons, and due to the activation of their CB1-Rs astrocytes release glutamate which activates NMDA receptors in neurons. Thus, because of its potential importance in pain processing we investigated the localization of CB1-Rs on astrocytes and microglial cells by using GFAP and CD11b as markers for astrocytes and microglial cells, respectively.

We obtained strong immunolabeling in the superficial spinal dorsal horn for both markers that was identical to that reported earlier. Investigating the co-localization between CB1-R and GFAP immunoreactivity, we found that 7.98 ± 0.57 and 9.66 ± 0.71% of CB1-R immunoreactive puncta were also stained for GFAP, whereas 45.61 ± 2.66 and 47.87 ± 1.42% of GFAP-immunoreactive profiles proved to be immunoreactive also for CB1-R in the medial and lateral aspects of the dorsal horn, respectively. In addition to GFAP, we revealed a substantial co-localization between CB1-R and CD11b immunoreactivities. Our co-localization figures showed that 10.42 ± 0.78 and 12.66 ± 1.27% of CB1-R-immunoreactive puncta were also stained for CD11b, whereas 70.27 ± 0.64 and 78.79 ± 1.23% of CD11b-immunoreactive profiles proved to be immunoreactive also for CB1-R in the medial and lateral aspects of the dorsal horn, respectively.

Distribution of CB1-receptors on the cell membrane of presynaptic axon terminals and glial processes

After revealing extensive co-localization between CB1-Rs and various axonal and glial markers, we intended to define the subcellular localization of CB1-receptors both in axon terminals and in glial profiles. Ultrathin sections immunostained according to the pre-embedding nanogold protocol for CB1-R were investigated at the ultrastructural level. Silver particles labeling CB1-Rs were recovered exclusively in axonal and glial-like profiles. No detectable staining was observed in dendrites or cell bodies of neurons. Immunoreactive axon terminals established both asymmetric and symmetric synaptic contacts. Immunoreactive axon terminals forming asymmetric and symmetric synaptic contacts contained spheroid and pleomorphic synaptic vesicles, respectively, but dense core vesicles were also revealed in some of the terminals with asymmetric synaptic apposition. Immunolabeled glial-like processes were frequently seen. In many cases, immunostained glial-like processes were revealed in close vicinity to synaptic contacts between immunoreactive axon terminals and postsynaptic dendrites. Regardless of whether the labeled profile was an axon terminal or glial-like profile, immunogold particles were revealed exclusively

in close association with the plasma membrane. The membrane- associated silver particles were found at the protoplasmic face of the plasma membrane, in agreement with the intracellular location of the epitope recognized by the antibody. The silver precipitates attached to the plasma membrane were distributed on extra-synaptic membrane compartments both close to and far from the synaptic apposition. None of them was recovered within the synaptic apposition.

Distribution of DGL-α and NAPE-PLD immunoreactivity in the superficial spinal dorsal horn

To elucidate the distribution of the DGL-α protein in laminae I–II of the spinal dorsal horn, immunostaining for DGL-α with an antibody directed against a long internal segment of the enzyme (residues 790–908) was carried out in the rat lumbar spinal cord. Both peroxidase-based and fluorescence single immunostaining revealed an abundant immunoreactivity for DGL-α throughout the superficial spinal dorsal horn. Lamina II appeared as a heavily stained band on the cross-section of the spinal cord, whereas lamina I and the deeper laminae of the dorsal horn were more sparsely stained. Immunostained elements appeared as punctate profiles both in the densely and sparsely stained zones. Besides the characteristic punctate labeling, larger immunoreactive spots resembling somata of neurons or glial cells were also scattered both in the gray and white matters.

To reveal immunonoreactivity for NAPE-PLD, sections of the lumbar spinal cord were reacted with a highly specific anti-NAPE-PLD antibody raised against the N-terminal 41 amino acids of the enzyme. Here, we observed a punctate immunostaining for NAPE-PLD, the density of which was more or less homogeneous throughout the entire cross-sectional area of the dorsal horn including laminae I and II. Similarly to DGL-α, larger NAPE-PLD immunoreactive spots resembling somata of neurons or glial cells were also observed.

Co-localization of DGL-α and NAPE-PLD immunoreactivity with markers of nociceptive primary afferents

As described earlier, most of the peptidergic nociceptive primary afferents express CGRP, whereas the cell membrane of the nonpeptidergic axon terminals binds IB4. Thus, to study the expression of DGL-α and NAPE-PLD on central axon terminals of peptidergic and nonpeptidergic

nociceptive primary afferents we investigated the co-localization of the enzymes with CGRP immunoreactivity and IB4-binding.

Investigating the co-localization between DGL-α and CGRP immunoreactivity, we collected 703 and 1,224 profiles immunostained for CGRP and DGL-α, respectively, and found that only 1.96±0.78% of DGL-a immunoreactive puncta were also stained for CGRP, whereas 3.41±1.11% of CGRP immunoreactive axon terminals proved to be immunoreactive also for DGL-α in laminae I–II of the dorsal horn. The co-localization values for NAPE-PLD were even lower. Following a careful analysis of 760 and 1,304 profiles immunostained for CGRP and NAPE-PLD, respectively, we found that 1.69±0.91% of NAPE-PLD immunoreactive puncta were also stained for CGRP, whereas 1.97±0.76% of CGRP immunoreactive axon terminals proved to be immunoreactive also for NAPE-PLD in the superficial spinal dorsal horn.

As it has been reported earlier, IB4-binding labeled a large number of axon terminals in lamina IIi. Despite the strong immunostaining and the substantial spatial overlap between the investigated profiles, the co-localization between axon terminals labeled with IB4-binding and puncta immunoreactive for DGL-α or NAPE-PLD was very low. After the investigation of 660 IB4-binding and 1,490 DGL-α immunostained profiles, it was found that 2.48±0.99% of DGL-α immunoreactive puncta were also positive for IB4-binding, whereas 1.06±0.79% of axon terminals that were positive for IB4-binding proved to be immunoreactive also for DGL-α. The co-localization values for NAPE-PLD were very similar. From 737 IB4-binding and 1,355 NAPE-PLD immunostained profiles 1.92±0.88% of NAPE-PLD immunoreactive puncta were also positive for IB4-binding, and 2.43±0.91% of axon terminals that were positive for IB4-binding proved to be immunoreactive also for NAPE-PLD in the superficial spinal dorsal horn.

Co-localization of DGL-α and NAPE-PLD immunoreactivity with markers of axon terminals of putative glutamatergic and GABAergic spinal neurons

As mentioned above, VGLUT2 can be used as a marker for axon terminals of intrinsic spinal neurons, whereas GABAergic neurons in the spinal cord contain both isoforms of GAD (GAD65 and GAD67). Therefore, to study the expression of DGL-α and NAPE-PLD on central axon terminals of putative glutamatergic and GABAergic spinal neurons we investigated co-localization between the enzymes and VGLUT2 as well as GAD65/67 immunoreactivities.

The co-localization values between the investigated enzymes and VGLUT2 immunoreactivity were slightly higher than were found for the co-localization with axon terminals of nociceptive primary afferents, but were still very low. Evaluating 725 and 1,508 profiles immunostained for VGLUT2 and DGL-α, respectively, we found that 3.78±0.59% of DGL-α immunoreactive puncta were also immunostained for VGLUT2, whereas 6.76±0.47% of axon terminals that were positive for VGLUT2 were also immunoreactive for DGL-α. The colocalization values for NAPE-PLD were even lower. In this case, after the investigation of 681 and 1,526 profiles immunostained for VGLUT2 and NAPE-PLD, respectively, it was revealed that 2.23±1.67% of NAPE-PLD immunoreactive puncta were also stained for VGLUT2, whereas 3.96±1.31% of VGLUT2 immunoreactive axon terminals proved to be immunoreactive also for NAPE-PLD.

Investigating the co-localization between DGL-α and GAD65/67 immunoreactivity, we collected 641 and 1,388 profiles immunstained for GAD65/67 and DGL-α, respectively, and found that 2.16±043% of DGL-α immunoreactive puncta were also stained for GAD65/67, whereas 3.12±0.93% of GAD65/67 immunoreactive axon terminals proved to be immunoreactive also for DGL-α. The co-localization values for NAPE-PLD were approximately similar. From 707 and 1,431 puncta immunostained for GAD65/67 and NAPE-PLD, respectively, 0.91±0.7% of NAPE-PLD immunoreactive puncta were also positive for GAD65/67, and 2.11±1.06% of axon terminals that were immunostained for GAD65/67 turned out also to be immunoreactive for NAPE-PLD in laminae I–II.

Co-localization of DGL-α and NAPE-PLD immunoreactivity with markers of astrocytes and microglial cells

Production and inactivation of endocannabinoids, anandamide and 2-AG, by cultured astrocytes and microglial cells have also been shown in many studies. Thus, because of the potential importance of endogenous cannabinoids in spinal pain processing we investigated the localization of DGL-α and NAPE-PLD on astrocytes and microglial cells by using GFAP and CD11b as markers for astrocytes and microglial cells, respectively.

Investigating the co-localization between DGL-α and GFAP immunoreactivity, we collected 216 and 1,321 profiles immunoreactive for GFAP and DGL-α, respectively, and found that 9.39±1.96% of DGL-α immunoreactive puncta also stained for GFAP, whereas 33.33±2.06% of GFAP immunoreactive profiles proved to be immunoreactive also for DGL-α. In addition to GFAP, we revealed a substantial co-localization between DGL-α and CD11b immunoreactivity. For the microglial marker, after the investigation of 207 and 1,297 profiles immunstained for CD11b and DGL-α, respectively, the co-localization analysis showed that 29.53±1.19% of DGL-α immunoreactive puncta were also stained for CD11b, whereas 67.15±2.21% of CD11b immunoreactive profiles were also immunoreactive for DGL-α.

The co-localization values between NAPE-PLD and the glial markers were very similar to the figures that we obtained for the co-localization between DGL-α and the same glial markers. However, there was a tendency for NAPE-PLD to have a slightly higher expression on glial cells than DGL-α. We collected 241 and 1,406 profiles immunoreactive for GFAP and NAPE-PLD, respectively, and found that 12.52±2.15% of NAPE-PLD immunoreactive puncta were also stained for GFAP, whereas 54.77±1.98% of GFAP immunoreactive profiles were also immunoreactive for NAPE-PLD in the superficial spinal dorsal horn. In addition, we investigated 223 and 1,501 profiles immunoreactive for CD11b and NAPE-PLD, respectively, and observed that 32.11±2.30% of NAPE-PLD immunoreactive puncta were also stained for CD11b, whereas 75.34±2.60% of CD11b immunoreactive profiles were immunoreactive for NAPE-PLD.

In order to substantiate the glial localization of the enzymes, in addition to the X-Y dimensions the confocal optical sections were also investigated in the X-Z and Y-Z projections. The X-Z and Y-Z images were drawn through the point of co-localization between the two markers, and the two orthogonal views were investigated for overlap.

Ultrastructural localization of DGL-α and NAPE-PLD immunoreactivity

Ultrathin sections immunostained for DGL-α and NAPE-PLD were investigated at the ultrastructural level. After finding a minimal overlap between immunolabeling for DGL-α and NAPE-PLD with various axonal markers and an extensive co-localization between DGL-α and NAPE-PLD with markers for astrocytes and microglial cells in double immunostained sections, we defined the subcellular localization of DGL-α and NAPE-PLD both in axon terminals and glial

profiles. Furthermore, since we recovered only approximately half of the DGL-α and NAPE-PLD immunoreactive puncta on axon terminals and glial cells in the co-localization studies, an extensive search for DGL-α and NAPE-PLD immunolabeling in the somatodendritic compartment of neurons was also carried out.

In agreement with the results obtained from the colocalization studies, peroxidase reaction precipitates and silver intensified nanogold particles labeling DGL-α and NAPE-PLD were recovered primarily in dendrites and glial processes and were found only occasionally in axon terminals.

Regardless of whether the labeled profile was a dendrite, glia-like process or an axon terminal, immunolabeling was revealed exclusively in close association to the plasma membrane. The membrane-associated immunoprecipitates and nanogold particles were found at the cytoplasmic face of the plasma membrane, in agreement with the intracellular location of the epitopes recognized by the antibodies. In dendrites, the end product of the immunoperoxidase and nanogold staining for DGL-α was observed at membrane compartments where the dendrites received synaptic contacts from axon terminals with different morphology, including boutons representing the central element of synaptic glomeruli.

Regardless of the morphology of the presynaptic axon, immunolabeling for DGL-α was always observed adjacent or in close vicinity to synaptic apposition. In case of the nanogold staining, silver intensified gold particles were found in perisynaptic position at asymmetric synaptic contacts. In the case of the immunoperoxidase staining, the immunoprecipitate also covered a part of the postsynaptic membrane.

Similar to DGL-α, immunolabeling for NAPE-PLD in dendrites also appeared as small immunoprecipitates associated with the inner surface of the cell membrane. However, these immunolabeled membrane compartments were never observed in close vicinity to synaptic appositions, although this finding may be limited by the fact that we investigated single and not serial ultrathin sections. In axon terminals, labeling was only occasionally found for either DGL-α or NAPE-PLD. In some cases the labeled membrane segments were adjacent to synaptic contacts, in other cases there was no sign of synaptic specialization in the vicinity of the labeled membrane compartments. We have to add, however, that we studied single and not serial ultrathin sections, thus the accurate relationship between the sites of labeling and synapses formed by the labeled axon terminal can not be definitively determined from our observations.

In glia-like processes, the labeling was abundant for both DGL-α and NAPE-PLD. Immunolabeled glia-like processes were frequently observed. It was a general finding that the membrane compartment immunureactive for DGL-α or NAPE-PLD was restricted only to a segment of the glial membrane, while the adjacent part of the glial profile was free of labeling. In the case of DGL-α, immunostained glia-like processes were frequently revealed in close vicinity to synaptic contacts between axon terminals and postsynaptic dendrites immunoreactive for DGL-α. In case of NAPE-PLD, however, dendritic segments immunoreactive for the enzyme were never observed in the vicinity of immunoreactive compartments of glia-like processes. Nevertheless, glia-like profiles immunostained for NAPE-PLD were sometimes revealed near to synapses. Unfortunately, we were not able to define whether the detected immunoprecipitates were in astrocytes or microglial cells, since we cannot make any distinction between the profiles of these glial cells in the electron microscope.

DISCUSSION

Investigating the cellular distribution of CB1-Rs in laminae I–II of the rat spinal dorsal horn with immunocytochemical methods, we revealed CB1-R-immunoreactive puncta exclusively on axon terminals and glial cells. Studying the localization of CB1-R on different populations of axon terminals, we found that nearly half of the peptidergic and slightly more than 20% of the non-peptidergic nociceptive primary afferent terminals were positively stained for CB1-R. Besides axon terminals of primary afferents, more than one-third and approximately 20% of the axon terminals of putative glutamatergic and GABAergic spinal interneurons were also immunoreactive for CB1-R, respectively. In addition to axonal expression, we also revealed a strong CB1-R immunostaining on glial cells. Almost half of the astrocytic and nearly 80% of microglial profiles was immunolabelled for CB1-R.

We also investigated the distribution of DGL-α and NAPE-PLD, enzymes involved in synthesizing the endocannabinoid ligands 2-AG and anandamide, respectively, in the superficial spinal dorsal horn of rats. Postsynaptic dendrites displayed strong immunolabeling for both enzymes, but positive staining was revealed only occasionally in axon terminals. Immunolabeling for DGL-a in dendrites was always revealed at membrane compartments adjacent to synapses. Dendritic membrane segments immunolabeled for NAPE-PLD, however, were never found to be associated with synapses. In addition to dendritic expression, both enzymes showed a remarkably strong expression on astrocytes and microglial cells.

CB1 receptors on central axon terminals of nociceptive primary afferents

The localization of CB1-Rs in central and peripheral neurons that are implicated in nociceptive processing and the discovery of putative endogenous suggested that an important function of the cannabinoid system is to modulate pain. It has been demonstrated that cannabinoids reduce behavioral responses to noxious stimuli. Furthermore, electrophysiological and neurochemical studies have provided convincing evidence that these anti-nociceptive actions are associated with cannabinoid-induced suppression of noxious stimulus-induced activity of neurons in the spinal cord. The suppression proved to be mediated at least partly by the activation of

presynaptic CB1-Rs expressed on central terminals of both C- and Aδ-type nociceptive primary afferents, thus decreasing the probability of glutamate release from nociceptive primary afferents.

Although the presence of functional CB1-Rs on spinal axon terminals of nociceptive primary afferents is well established, how many of them express CB1-R is still a matter of debate. Experimental evidence indicates that dorsal rhizotomy resulted in only a marked decrease in CB1-R immunoreactivity, however, it has also been demonstrated that dorsal rhizotomy induced a 50% loss in binding of cannabinoid agonists in laminae I–II. Physiological findings also indicate that a substantial proportion of nociceptive primary afferents respond to endogenous cannabinoid release in the spinal cord. C and Aδ fiber-evoked monosynaptic excitatory postsynaptic currents (EPSCs) can be depressed by CB1-R agonist in nearly one-third and two-thirds of spinal neurons, respectively.

Our present quantitative evaluation concerning the distribution of CB1-R-immunoreactive puncta in the superficial spinal dorsal horn has shed new light on this issue. On the one hand, we revealed that nearly half of the peptidergic and slightly more than one-fifth of the non-peptidergic nociceptive primary afferent axon terminals express CB1-Rs on their cell membrane. These values are in good agreement with earlier physiological observations and binding studies. However, it is also essential to note that we were not able to detect CB1-Rs on at least half of the peptidergic and 80% of the nonpeptidergic axon terminals of nociceptive primary afferents, indicating that the magnitude of presynaptic cannabinoid modulation of different nociceptive inputs conducted by different sets of nociceptive primary afferents may vary over a wide range, from very strong to none. What these types of nociceptive signals are, and what types are not controlled by presynaptic cannabinoid mechanisms will be the subjects of future studies.

CB1 receptors on axon terminals of spinal neurons

In good agreement with our present results, autoradiographic studies in rats treated with neonatal capsaicin suggested that only 16% of spinal CB1-Rs are located on C-fiber afferent endings suggesting that a substantial proportion of CB1-Rs are likely to be expressed on intrinsic interneurons in the superficial spinal dorsal horn. Reinforcing this notion, expression of CB1-R mRNA and immunoreactivity for CB1-R have been reported in all spinal laminae including the superficial spinal dorsal horn where functional studies demonstrated CB1-R-mediated presynaptic inhibition of both GABAergic and glutamatergic transmission.

Although the expression of functional CB1-Rs on spinal neurons is generally accepted, the distribution of CB1-Rs on the somatodendritic and axonal membrane compartments of spinal dorsal horn neurons is still far from completely known. In most morphological studies available, CB1-Rs were revealed within the somata and dendrites of spinal interneurons. In contrast, the application of endogenous cannabinoids onto spinal cord preparations has been shown to evoke responses that are likely to be mediated by presynaptic CB1-Rs. The present results strongly reinforce the findings obtained from physiological studies. Without obtaining any somato-dendritic staining, we encountered CB1-R-immunoreactive puncta on axon terminals of putative glutamatergic and GABAergic spinal interneurons in large numbers. However, similar to axon terminals of primary afferents only a proportion of axon terminals of intrinsic spinal neurons proved to be immunoreactive for CB1-Rs. We were not able to detect CB1-Rs in more than 60 and 80% of axon terminals of putative glutamatergic and GABAergic neurons, respectively, in laminae I–II of the spinal gray matter, indicating that a pre-synaptic cannabinoid mechanism may modulate only some of the excitatory and inhibitory interactions among spinal neurons. This conclusion appears to be well supported by the present results, although the proportion of CB1-R expressing and non-expressing axon terminals of putative glutamatergic spinal neurons may have been slightly miscalculated as some of the VGLUT2-immunoreactive boutons may represent axon terminals of primary afferents.

CB1 receptors on glial cells

It has recently become generally accepted that there are bidirectional communication pathways between glial cells and neurons in the central nervous system. Endocannabinoid-mediated neuron–astrocyte as well as neuron–microglial cell signaling has also been reported. It has been demonstrated, that hippocampal astrocytes express CB1-Rs, activation of which lead to phospholipase C-dependent Ca^{2+} mobilization from internal stores. The increased Ca^{2+} level stimulates glutamate release from the astrocytes that activates NMDA receptors in pyramidal neurons. CB1-Rs expressed by microglial cells in the cerebral cortex also appear to be functionally relevant. They have been implicated as linked to the modulation of chemokine and cytokine expression in the central nervous system. In addition to telencephalic structures, the expression of CB1-Rs by astrocytes has also been demonstrated in the superficial spinal dorsal horn.

In agreement with previous studies, here we demonstrated that half of the astrocytic and 80% of microglial profiles express CB1-Rs in laminae I–II of the spinal dorsal horn. There is general agreement that glial cells in the spinal dorsal horn can powerfully control pain when they are activated to produce various pain mediators.

Although the significance of glial CB1-Rs in spinal nociceptive information and pain processing is far from being understood, it is likely that similarly to their reported function in the hippocampus and cerebral cortex they may modulate chemokine, cytokine or glutamate release, and might also be involved in other signaling mechanisms in the superficial spinal dorsal horn. Nevertheless, the fact that astrocytes and microglial cells express CB1-Rs in the superficial spinal dorsal horn must be considered when interpreting the cellular basis of the effects of cannabinoids on pain behavior.

DGL-α and NAPE-PLD in axon terminals

We found only occasional immunolabeling for DGL-α in axon terminals of multiple origins in the superficial spinal dorsal horn. This observation is in good agreement with the results of recent morphological studies confirming that DGL-α is primarily localized in postsynaptic dendrites that face CB1-R expressing terminals.

Our present findings concerning the scanty appearance of NAPE-PLD in axon terminals, however, do not harmonize so well with earlier reports. Authors of some recent articles noted that in higher brain centers NAPE-PLD is concentrated presynaptically in several types of excitatory axon terminals, where it is localized predominantly on the intracellular membrane cisternae of axonal calcium stores. The expression of NAPE-PLD in the cell bodies of primary sensory neurons within dorsal root ganglia (DRG) has also been reported. In contrast to this, we observed unexpectedly low levels of NAPE-PLD immunolabeling in axon terminals in the superficial spinal dorsal horn. This finding suggests that the NAPE-PLD protein is transported from the perikarya of DRG and spinal neurons to their spinal axon terminals in such a limited amount that it is below the threshold of immunocytochemical detection, indicating that the synthesis of anandamide (or other acyl amines) in axon terminals of the dorsal horn by NAPE-PLD may not be very prominent.

Differential distribution of DGL-α and NAPE-PLD in dendrites

There is general agreement in the literature that 2-AG is released from postsynaptic neurons in an activity dependent manner, travels retrogradely through the synaptic cleft, engages presynaptic CB1-Rs, which then suppress neurotransmitter release from glutamatergic axon terminals. Variations in this basic scheme accounts for numerous forms of short- and long-term synaptic plasticity and experience-dependent modifications of neuronal activity in the central nervous system. Our present results concerning the perisynaptic dendritic distribution of DGL-α are fully consistent with these previous findings.

In contrast to the well-established distribution and functional properties of 2-AG-mediated retrograde signaling, the molecular architecture underlying the synthetic side of the anandamide-related endocannabinoid system remains largely unknown, although endogenous anandamide has often been implicated in various behaviors, such as emotion, learning, or pain. In addition, even the sparsely available data addressing the organization of anandamide-related molecular machineries are controversial. As mentioned earlier, most authors have found that NAPE-PLD is concentrated presynaptically in several types of excitatory axon terminals. Others, however, argue in favor of a somatodendritic localization of NAPE-PLD. Our present findings clearly support the idea of dendritic localization of NAPE-PLD in the superficial spinal dorsal horn.

DGL-α and NAPE-PLD in glial cells

The expression of functional CB1-Rs by astrocytes and microglial cells has been reported. It has also been demonstrated that astrocytes and microglial cells have the potential to produce 2-AG and anandamide and thus can communicate with neighboring neurons through endocannabinoid signaling. Endocannabinoid mediated astrocyte-neuron as well as microglial cell-neuron signaling has indeed been reported. Our present results demonstrating an abundant expression of DGL-α and NAPE-PLD in both astrocytes and microglial cells provide further evidence for possible communication pathways between glial cells and neurons, as well as between glial cells in the spinal dorsal horn.

A proposed scheme for the endocannabinoid mechanisms in the superficial spinal dorsal horn

In the superficial spinal dorsal horn, the primary activation of neurons in laminae I–II arises from nociceptive primary afferents, which is necessary to induce the activity dependent endocannabinoid mobilization. Spinal neurons activated by glutamatergic nociceptive primary afferent inputs may release 2-AG from perisynaptic and anandamide from extrasynaptic dendritic membrane compartments. The released endocannabinoids may diffuse out from their site of mobilization and activate CB1-Rs on axon terminals of primary afferents as well as spinal interneurons resulting in temporary impairment of neurotransmitter release from the CB1-R expressing axon terminals. The endocannabinoid-induced decrease in the probability of neurotransmission either from primary afferents or intrinsic spinal neurons may deeply influence the function of the spinal pain processing neural network.

In addition to neurons, astrocytes and microglial cells also express CB1-Rs, which may also be activated by the postsynaptically released endogenous cannabinoids resulting in phospholipase C-dependent Ca^{2+} mobilization from cytoplasmic stores. In turn, the increased Ca^{2+} level may activate DGL-α and NAPE-PLD resulting in the release of 2-AG and anandamide from glial cells. The released endocannabinoids may diffuse out and, together with 2-AG and anandamide released by dendrites, may act on neural CB1-Rs affecting functional properties of spinal neurons remote from their site of release. Alternatively, $G_{q/11}$-linked GPCRs expressed on astrocytes and microglia may also drive glial endocannabinoid production.

Although the way how the glial endocannabinoid system contributes to nociceptive functions remains to be elucidated, the fact that astrocytes and microglial cells express functional CB1-Rs, DGL-a and NAPE-PLD must be considered in the interpretation of effects of cannabinoids on spinal pain processing; especially in chronic pain when the number and activity of microglial cells and astrocytes are substantially increased.

SUMMARY

A long line of experimental evidence indicates that endogenous cannabinoid mechanisms play important roles in nociceptive information processing in various areas of the nervous system including the spinal cord. In our experiments, using immunocytochemical methods at the light and electron microscopic levels, we investigated the cellular distribution of type-1 cannabinoid receptor (CB1-R), and the two major endocannabinoid-synthesizing enzymes, diacylglycerol lipase alpha (DGL-α) and N-acylphosphatidylethanolamine-specific phospholipase D (NAPE-PLD) in laminae I and II of the rodent spinal dorsal horn.

Axonal varicosities revealed a strong immunoreactivity for CB1-R, but no CB1-R expression was observed on dendrites and perikarya of neurons. Investigating the co-localization of CB1-R with markers of peptidergic and non-peptidergic primary afferents, and axon terminals of putative glutamatergic and GABAergic spinal neurons we found that nearly half of the peptidergic (immunoreactive for calcitonin gene-related peptide) and more than 20% of the non-peptidergic (binding isolectin B4) nociceptive primary afferents, more than one third and approximately 20% of the axon terminals of putative glutamatergic (immunoreactive for vesicular glutamate transporter 2) and GABAergic (immunoreactive for glutamic acid decarboxylase; GAD65 and/or GAD67) spinal interneurons, respectively, were positively stained for CB1-R. In addition to axon terminals, almost half of the astrocytic (immunoreactive for glial fibrillary acidic protein) and nearly 80% of microglial (immunoreactive for CD11b) profiles were also immunolabeled for CB1-R.

In contrast to the abundant axonal distribution of CB-Rs, immunoreactivities for DGL-α and NAPE-PLD were primarily associated with dendrites in the spinal dorsal horn, while axon terminals showed positive labeling only occasionally. However, the dendritic localization of DGL-α and NAPE-PLD showed a remarkably different distribution. DGL-α immunolabeling in dendrites was always revealed at membrane compartments in close vicinity to synapses. In contrast to this, dendritic NAPE-PLD labeling was never observed in association with synaptic contacts. In addition to dendrites, a substantial proportion of astrocytic (immunoreactive for GFAP) and microglial (immunoreactive for CD11b) profiles were also immunolabeled for both DGL-α and NAPE-PLD. Glial processes immunostained for DGL-α were frequently found near to synapses in which the postsynaptic dendrite was immunoreactive for DGL-α, whereas NAPE-PLD immunoreactivity on glial profiles at the vicinity of synapses was only occasionally observed.

Our results suggest that both neurons and glial cells can synthesize and release 2-AG and anandamide in the superficial spinal dorsal horn. 2-AG can primarily be released by postsynaptic dendrites and glial processes adjacent to synapses, whereas anandamide can predominantly be released from nonsynaptic dendritic and glial compartments. The activity-dependent release of endogenous cannabinoids may activate a complex signaling mechanism in the pain processing spinal neural circuits into which both neurons and glial cells may contribute.

Register Number: DEENKÉTK/162/2013.
Item Number:
Subject: Ph.D. List of Publications

Candidate: Zoltán Hegyi

Neptun ID: PC5PRJ

Doctoral School: Doctoral School of Neurosciences

List of publications related to the dissertation

1. **Hegyi, Z.**, Holló, K., Kis, G., Mackie, K., Antal, M.: Differential distribution of diacylglycerol lipase-alpha and N-acylphosphatidylethanolamine-specific phospholipase D immunoreactivity in the superficial spinal dorsal horn of rats.
   Glia. 60 (9), 1316-1329, 2012.
   DOI: http://dx.doi.org/10.1002/glia.2235
   IF:4.82 (2011)

2. **Hegyi, Z.**, Kis, G., Holló, K., Ledent, C., Antal, M.: Neuronal and glial localization of the cannabinoid-1 receptor in the superficial spinal dorsal horn of the rodent spinal cord.
   Eur. J. Neurosci. 30 (2), 251-262, 2009.
   DOI: http://dx.doi.org/10.1111/j.1460-9568.2009.06816.x
   IF:3.418

List of other publications

3. Karosi, T., Csomor, P., **Hegyi, Z.**, Sziklai, I.: The presence of CD209 expressing dendritic cells correlates with biofilm positivity in chronic rhinosinusitis with nasal polyposis.
   Eur. Arch. Oto-Rhino-Laryn. Epub ahead of print (2013)
   DOI: http://dx.doi.org/10.1007/s00405-013-2372-9
   IF:1.287 (2011)

4. Szalai, E., Felszeghy, S., **Hegyi, Z.**, Módis, L., Berta, A., Kaarniranta, K.: Fibrillin-2, tenascin-C, matrilin-2, and matrilin-4 are strongly expressed in the epithelium of human granular and lattice type I corneal dystrophies.
Mol. Vis. 18, 1927-1936, 2012.
IF:2.205 (2011)

Total IF: 11.73

Total IF (publications related to the dissertation): 8.238

The Candidate's publication data submitted to the Publication Database of the University of Debrecen have been validated by Kenezy Life Sciences Library on the basis of Web of Science, Scopus and Journal Citation Report (Impact Factor) databases.

02 May, 2013

Conference abstracts

1. **Hegyi Z**, Kis G, Antal M: Neuronal and glial localization of the cannabinoid-1 receptor in the superficial dorsal horn of the rodent spinal cord. *IBRO International Workshop*, Debrecen, 2008.
2. **Hegyi Z**, Kis G, Holló K, Ledent C, Antal M: Neuronal and glial localization of the cannabinoid-1 receptor in the superficial dorsal horn of the rodent spinal cord. *6th FENS Forum*, Geneva, 2008.
3. **Hegyi Z**, Antal M: Reorganization of cannabinoid-1 receptor expression in the superficial spinal dorsal horn of rats in inflammatory pain. *Annual Conference of the Hungarian Neuroscience Society*, 2008.
4. **Hegyi Z**, Holló K, Kis G, Mackie K, Antal, M: Differential distribution of DGL-alpha and NAPE-PLD immunoreactivity in the superficial spinal dorsal horn of rodents. *IBRO Workshop*, Pécs, 2010.
5. **Hegyi Z**, Kis G, Holló K, Ledent C, Mackie K, Antal M: Differential distribution of CB1 receptor, DGL-alpha and NAPE-PLD immunoreactivity in the superficial spinal dorsal horn of rodents. *Workshop on the endocannabinoid system*, Bonn, 2010
6. **Hegyi Z**, Kis G, Holló K, Mackie K, Antal M: Differential distribution of DGL-alpha and NAPE-PLD immunoreactivity in the superficial spinal dorsal horn of rodents. *FENS Forum*, 2010, Amsterdam
7. **Hegyi Z**, Kis G, Holló K, Mackie K, Antal M: Differential distribution of diacylglycerol lipase-alpha and N-acyl-phosphatidyl-ethanolamine-hydrolyzing phospholipase D immunoreactivity in the superficial spinal dorsal horn of rodent. *Joint Conference of the LXXV. Meeting of the Hungarian Physiological Society with participation of the Hungarian Society of Anatomists, the Experimental Section of the Hungarian Society for Experimental and Clinical Pharmacology and the Hungarian Society for Microcirculation and Vascular Biology*, Pécs, 2011.
8. **Hegyi Z**, Holló K, Antal M: Co-expression of CB1 receptors and the major endocannabinoid-synthesizing enzymes, DGL-α and NAPE-PLD by astrocytes in the rat spinal cord. *FENS Forum*, 2012, Barcelona

9. Holló K, Ducza L, Bakk E, Hegedus K, **Hegyi Z**, Antal M: Expression And Cellular Localization Of Interleukin-1 Receptor Type-1 In The Spinal Dorsal Horn In The Freund Adjuvant-Evoked Inflammatory Pain. *FENS Forum*, 2012, Barcelona
10. **Hegyi Z**, Oláh T, Docova K, Holló K, Csernoch L, Antal M: Endocannabinoid-mediated calcium signaling in spinal astrocytes. *Annual Conference of the Hungarian Neuroscience Society*, 2013, Budapest
11. Holló K, Gajtkó A, Hegedűs K, Bakk E, **Hegyi Z**, Antal M: IL-1 beta production by cultured spinal cord astrocytes upon LPS treatment is influenced by ATP and glutamate. *Annual Conference of the Hungarian Neuroscience Society*, 2013, Budapest
12. Docova K, **Hegyi Z**, Holló K, Kis G, Mackie K, Antal M: Distribution of monoacylglycerol lipase (MGL) immunoreactivity in the superficial spinal dorsal horn of rodents. *Annual Conference of the Hungarian Neuroscience Society*, 2013, Budapest